An Amplitude Variation-Based Hydrocarbon Detection Method for Coal-Underlying Tight Sandstone

Xi Wang[1], Gang Zhao[1], Qihai Nie[1], Yilan Meng[1], and Shang Xu[1]

[1]Overseas Business Department of Geophysical Research Institute, BGP, CNPC

Extended abstract

When post-stack seismic data is used for hydrocarbon detection in coal-bearing strata, it is crucial to determine the effect and extent of the coal layer on the reflection characteristics of underlying formations.

Forward modeling analysis indicates that the amplitude of tight gas reservoirs is generally weaker than that of dry layers. However, when affected by overlying coal layers, the amplitude of tight gas reservoir becomes stronger. This amplitude variation serves as a basis for hydrocarbon detection in coal-bearing strata. Based on these findings, this paper proposes three hydrocarbon detection methods that are applicable to coal-underlying tight sandstone. The first method involves waveform reconstruction to filter out the reflection of coal layers in seismic data. By calculating the ratio of the amplitude of tight sandstone before and after waveform reconstruction, potential gas-bearing zones with enhanced amplitude that influenced by the coal layer can be identified. The second method is based on calculating the absorption attenuation coefficient of the coal layer.

This coefficient is then used for deconvolution to obtain the events of tight sandstone before being influenced by coal layers. By analyzing the amplitude variation of the sandstone, potential gas-bearing zones can be

predicted. The third method is applicable when the total thickness of the underlying shale and tight sandstone is between 1/4 and 1/2 wavelength. This method utilizes the dual parameters of coal layer thickness and sandstone amplitude for hydrocarbon detection. The principle is to generate the trend line of gas-bearing sandstone based on the amplitude influence factor of coal layers. The inverse distance weighting algorithm is used to represent the probability of hydrocarbon content in the coal-underlying tight sandstone reservoirs. The gas-bearing sandstone trend line is then applied in the crossplot of coal thickness and amplitude of coal- underlying tight sandstone. The closer the prediction point is to the trend line in the crossplot, the higher the probability of a gas-bearing reservoir. In general, both the waveform reconstruction and coal layer absorption attenuation coefficient methods are based on the theories of seismic wave propagation and signal processing.

By calculating the amplitude difference of the coal-underlying tight sandstone reservoir before and after filtering out the coal layer reflections in post-stack seismic data, the hydrocarbon content of the underlying tight sandstone reservoir can be predicted based on the characteristic of enhanced amplitude after gas pooling in the tight sandstone. Although a portion of effective seismic signals may be lost after filtering out the coal layers, the advantage of these two methods lies in their wide applicability. The amplitude influence factor method is based on statistical-probabilistic theory. According to geological observation, this method allows for adjustments of

the gas-bearing sandstone trend line of the crossplot, making it more controllable in terms of quality. However, this method is limited in terms of its applicability conditions. These three methods provide effective approaches for hydrocarbon detection in coal-underlying tight sandstone, contributing to the exploration and development of oil and gas resources.

Keywords: Amplitude influence factor, Hydrocarbon probability distribution Chart, Gas bearing sandstone trend line, Absorption attenuation coefficient, Seismic waveform decomposition and reconstruction

0 Introduction

With the continuous increase in energy demand and the growing challenges in conventional oil and gas exploration, the proportion of unconventional oil and gas reservoirs is steadily increasing. This trend is particularly prominent in the realm of secondary exploration in oil fields. Tight sandstone gas reservoirs, being considered relatively accessible unconventional oil and gas resources, have emerged as a major focal point in global oil and gas exploration[1]. Significant progress has been made in the exploration of tight sandstone oil and gas reservoirs in western China. However, the intricate interplay between oil, gas, and water frequently leads to notable disparities in well productivity. Therefore, the detection of oil and gas is vital for pinpointing favorable locations within tight sandstone reservoirs. The Middle and Lower Jurassic coal-bearing strata are prevalent in Central Asia and extensively present in the northwest region of China. Noteworthy discoveries have been made in the Junggar Basin, Tuha Basin, Tarim Basin, Yanqi Basin, and Kuqa Depression[2], establishing them as important oil and gas-bearing strata. Long-term research has revealed that the Middle and Lower Jurassic coal seams and the associated organic-rich shales are significant source rocks in the southern Junggar Basin, northern Tarim Basin, and Tuha Basin. These formations are key layers for unconventional oil and gas exploration in these basins, highlighting the importance of studying coal-bearing strata. Understanding and utilizing the strong energy shielding effect of coal seams in these formations is essential for effective oil and gas detection. This knowledge is crucial for identifying geological sweet spots for the exploration of tight sandstone oil and gas reservoirs.

1 Background

This article focuses on the research which is conducted in the coal-bearing strata of Xishanyao Formation in the Middle Jurassic of Qiudong Sag of the Tuha Basin. The Qiudong Sag is located within the Taibei Depression, where high-yield tight sandstone oil and gas reservoirs have been discovered in the Lower Jurassic Sangonghe Formation. The Xishanyao Formation, which overlies the Sangonghe Formation, contains similar reservoir with those in the lower part of Sangonghe Formation, and it indicates significant exploration potential. Long-term studies indicate that the Taibei Depression is the primary subsidence area in the Tuha Basin and serves as the main oil and gas-bearing unit[3,4]. The analysis indicates that the primary cause of tight sandstone in the Qiudong Sag is linked to the development of the Shuixigou Group coal-bearing strata. During its formation, the diagenesis of sandstone underwent a slightly acidic environment with active chemical processes. Early strong compaction and pressure dissolution processes contributed to the rapid densification of the sandstone.

Furthermore, the deeper burial environment resulted in even denser reservoirs. Core data from drilling experiments reveal that the current porosity is predominantly less than 6% and permeability is mostly less than 0.1×10-3 um2, underscoring the overall poor reservoir properties. Previous research findings have highlighted the high quality of source rock of Shuixigou group in the Jurassic of Qiudong Sag. The various tectonic movements during the Yanshanian-Himalayan periods significantly influenced the structural, sedimentary, and hydrocarbon accumulation in the Jurassic-Cretaceous strata. Tectonic evolution analysis reveals that during the early Yanshanian period, the initial development of the anticline structure in the Qiudong Sag emerged. The first phase of the Yanshan Movement led to uplift and thrusting in the northern Bogda Mountains and multiple reverse faults formed formed in the lower depression area during the Middle- Lower Jurassic. In the late Jurassic Yanshan Movement phase II, the lower depression area experienced differential thrusting, resulting in local structural uplift. The

Yanshan Movement phase III-Himalayan period marked the primary hydrocarbon expulsion phase in the region. As the differential thrusting in the lower depression area gradually decreased, compression activities in a near north-south direction impacted the study area, leading to the gradual formation of the current north-south high, central low, and wide gentle anticline structure in the east-west direction. Sedimentary analysis indicates that the Qiudong Sag experienced dual- source sedimentation from the north and south, and underwater distributary channel of braided river delta front is the main sedimentary micro-facies. In the southern provenance direction, syn-sedimentary folding activities led to the development of secondary folds, resulting in the formation of "full depression rich sand" below the slope. This area, where oil and gas are preferentially charged near the source, facilitates the formation of primary oil and gas reservoirs. Drilling data suggests that the structural trapping mechanism of tight oil and gas reservoirs in lower position of the depression is relatively weak. To enhance reserves, a key study which focuses on the tight oil and gas reservoirs in the extensive hydrocarbon-rich depressions is to identify sweet spots with relatively high oil and gas content in the coal-bearing strata of the Xishanyao Formation.

2 Technology

During the propagation of elastic wave signals in the formation, discontinuous interfaces between layers can lead to attenuation and dispersion of elastic waves. Larger interfaces result in stronger dispersion, causing the peak frequency to shift towards lower frequencies as the waves penetrate. In coal-bearing strata, the relatively low impedance of coal seams causes seismic waves passing through them to experience an increase in impedance and a decrease in frequency at the interface. This interference disrupts the reflection characteristics of the underlying strata, particularly affecting the ability of seismic data to identify reservoirs and their oil and gas content. To investigate the impact of coal seams on the underlying strata and its extent, this study developed corresponding forward models based on actual well data.

2.1 Forward modeling analysis

A 1D forward modeling study was conducted to assess the impact of coal seams on underlying formations, utilizing actual drilling data. In Figure 1, the initial column displays the lithology logged in a gas-producing well, indicating the presence of a 40m coal seam. The three red curves on the right depict the square wave transformation of longitudinal wave impedance curves, enabling the determination of impedance values for the water layer, gas layer, and dry layer beneath the coal seam through fluid substitution. The subsequent three synthetic logging traces illustrate the results of 1D forward modeling for the water layer, gas layer, and dry layer of the tight sandstone reservoir under the 40m coal seam, with a more pronounced amplitude observed for the gas layer that was compared to the dry layer. The middle set of impedance and synthetic logs represent the 1D forward modeling outcomes for the water layer, gas layer, and dry layer of the tight sandstone reservoir under a 20m coal seam. The set of impedance and synthetic logs on the right demonstrate the 1D forward modeling results for the water layer, gas layer, and dry layer of the tight sandstone reservoir in the absence of coal seam development, revealing notably weaker amplitude for the gas layer compared to the dry layer. Overall, the 1D forward modeling analysis indicates that the seismic reflection of the gas layer and dry layer within the tight sandstone reservoir undergoes significant changes when influenced by overlying coal seams.

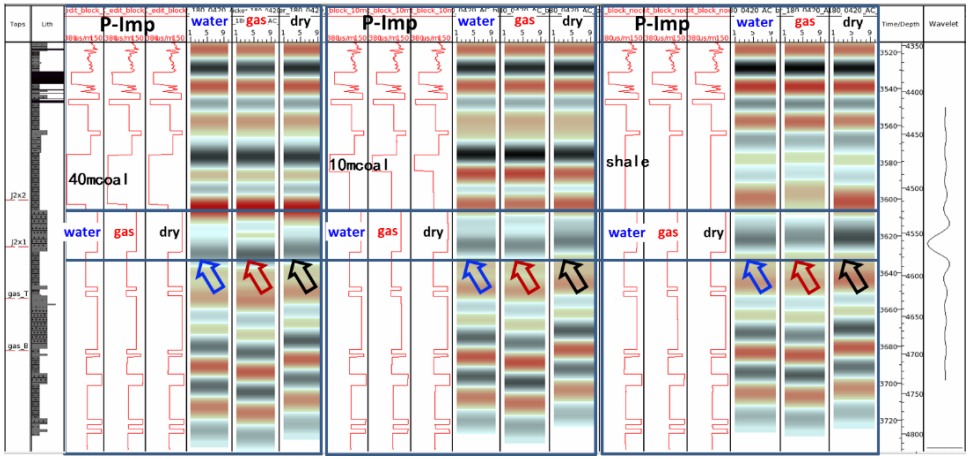

Figure 1 A comparison of the 1D forward modeling results under various coal seam conditions.

Figure 2 shows 2D forward modeling results of the tight sandstone reservoir with different fluids. The velocities and densities utilized in the forward modeling are based on the well logging data from this depression. In Figures 2(a) and 2(b), the comparison of forward modeling results for the water layer, gas layer, and dry layer under a shale background reveals weakest amplitude for the gas layer and strongest amplitude for the dry layer. Figures 2(c) and 2(d) illustrate the comparison of forward modeling results for the water layer, gas layer, and dry layer of the tight sandstone reservoir under the coal seam, demonstrating that the gas layer exhibits stronger amplitudes compared to the dry layer. The 2D forward modeling outcomes align with the 1D results, providing further evidence that the presence of coal seam influence leads to a significant increase in the amplitude of gas- bearing reservoirs within tight sandstone reservoirs.

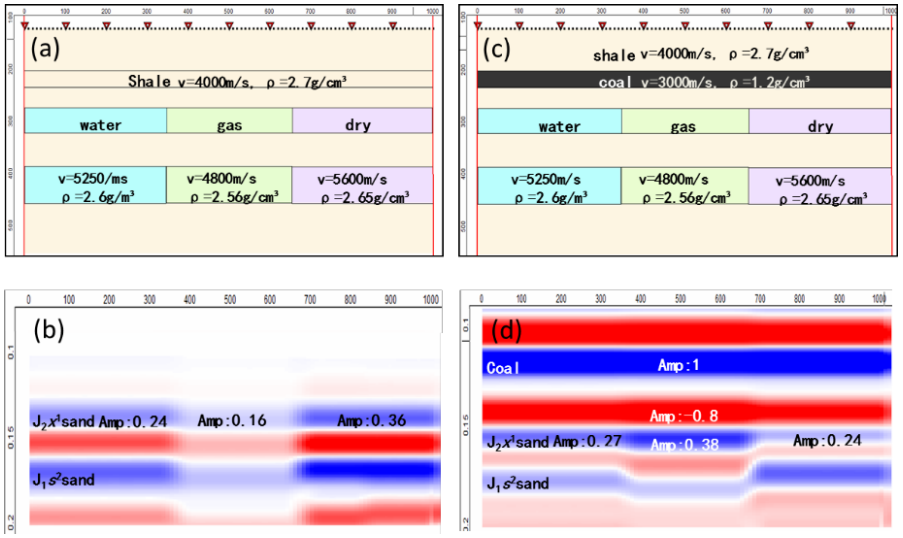

Figure 2 The 2D forward modeling of the tight sandstone reservoir with different fluids based on existing drilling information. Panel (a) shows the geological model without coal seam development, while panel (b) displays the forward modeling results under the same condition. Panel (c) presents the geological model under a 40m coal seam, and panel (d) show cases the forward modeling results under the influence of a 40m coal seam.

To elucidate the reasons behind the aforementioned forward modeling results and determine the extent of coal seam influence on the underlying formations, this study further dissected the lithological combinations and conducted forward modeling analysis. Figure 3 provides a comparison of 1D forward modeling results under various lithological combination conditions. The leftmost group in the figure illustrates the original logging lithology of a gas-producing well, revealing the presence of a 40m coal seam with a tight sandstone reservoir beneath it. The first and second columns of synthetic seismograms depict the seismic reflections of the gas layer and dry layer underlying the 40m coal seam, with the forward modeling curves of the gas layer and dry layer derived through fluid replacement. The middle showcases the reflection when only shale exists beneath the 40m coal seam, aiming to observe the wave impedance interface generated by the coal seam. The rightmost group in the figure displays the reflections of the gas layer and dry layer in the tight sandstone reservoir in the absence of the coal seam, indicating that the amplitude of the dry layer is stronger than that of the gas layer. The forward modeling results suggest that the interference at the top boundary of the coal seam and the reflection at the bottom boundary create a stronger trough reflection at the position of the underlying tight sandstone. When this strong trough reflection overlaps with the peak reflection of the sandstone, it leads to the waveform change and an increase in gas layer amplitude and a decrease in dry layer amplitude. Furthermore, the figure demonstrates that the influence range of the coal seam on the underlying formations is approximately 90m.
Based on the seismic characteristics of the study area and the forward modeling wavelet, it is inferred that the influence range of the coal seam on the underlying formations is approximately equivalent to half a wavelength.

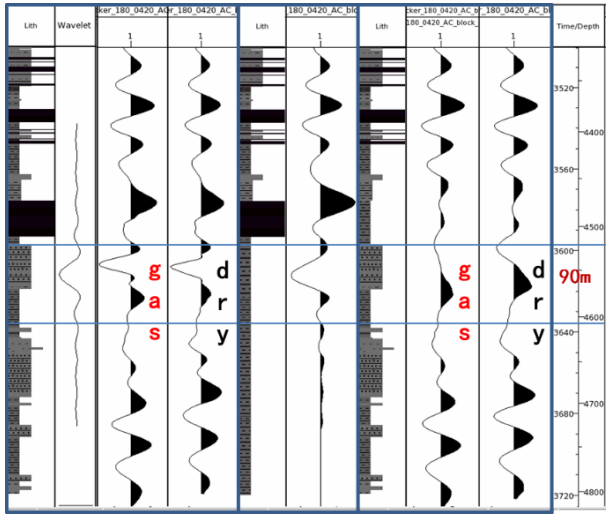

Figure 3 Comparison of 1D forward modeling results under various lithological combination.

2.2 Post-stack hydrocarbon detection based on the amplitude influence factor of coal seams

2.2.1 Theoretical Framework

Previous studies on coal-bearing strata based on seismic data mainly focused on the suppression and filtering of coal seams. However, there is a lack of widely applicable research examples for post-stack hydrocarbon detection using coal seam effects. This paper introduces a post-stack oil and gas detection method that is based on the amplitude influence factor of coal seams. The principle of this method is that the influence of coal seams on underlying sandstones varies with the thickness of the coal seams. Through the utilization of well data and forward modeling, the amplitude influence factor of coal seams on underlying sandstones can be calculated.

In general, the amplitude of reservoirs beneath coal seams is influenced by four main factors: coal seam thickness, thickness of shale beneath the coal, thickness of tight sandstone, and the status of oil and gas within these layers. The statistical results of forward modeling under different conditions of coal seam thickness, shale thickness beneath the coal, sandstone thickness beneath the coal, and various fluid statuses are presented in Table 1. The forward modeling results reveal that when the thickness beneath the coal is 20m, the amplitude of the gas layer significantly increases as the sandstone thickness reaches 70m and 100m, while the dry layer amplitude is stronger at 20m. When the shale thickness beneath the coal is 40m and the sandstone thickness is 20m, the gas layer amplitude is stronger than the dry layer, but the dry layer amplitude significantly increases when the sandstone thickness exceeds 50m. With an 80-meter mudstone thickness beneath the coal seam, dry layer amplitudes are generally stronger, indicating that the reservoir is less affected by the coal seam.

Based on the comprehensive forward modeling results, it is concluded that when the total thickness of shale beneath the coal and tight sandstone is greater than 1/4 wavelength and less than 1/2 wavelength, the amplitude of gas-bearing reservoirs is relatively stronger. In such cases, the amplitude influence factor of coal seams can be utilized for oil and gas detection using a “dual-parameter” approach which is based on coal seam thickness and sandstone amplitude. The principle involves using distance to represent the probability of oil and gas in the reservoir beneath the coal, where the points that are closer to the “gas-bearing sandstone trend line” indicate a higher probability of gas-bearing. Subsequently, the reservoir’s probability of gas bearing can be calculated using a reverse distance weighting algorithm.

The formula for the “gas-bearing sandstone trend line” is:

$$y=(ax+b)*(-3E\text{-}07x^4 + 7E\text{-}05x^3 - 0.007x^2 + 0.2671x - 3)$$

In the formula, x represents the thickness of coal seams, and y represents the amplitude of tight sandstone beneath the coal. In order to illustrate the significant variation of amplitude across different study areas and versions of seismic data, non-dimensional parameters “a” and “b” are incorporated to adjust the shape of the trend line, ensuring its adaptability to different areas.

Table 1 The statistical results of multivariate forward modeling in coal-bearing strata

Coal Thickness	0			20			30			40			60			80		
Lith	Water	Gas	Dry	Water	Gas	Dry	Water	Gas	Dry	Water	Gas	Dry	Water	Gas	Dry	Water	Gas	Dry
20m Shale																		
20m Sand	0.38	0.2	0.81	0.65	0.48	0.6	0.92	0.69	0.88	1.14	0.97	1.16	1.2	1.05	1.25	0.1	0.2	0.02
50m Sand	0.57	0.25	0.86	0.14	0.09	0.53	0.45	0.32	0.56	0.62	0.56	0.65	0.89	0.74	0.91	0.08	0.36	0.05
70m Sand	0.06	0.1	0.07	0.52	0.43	0.3	0.77	0.63	0.55	0.9	0.87	0.69	0.89	0.91	0.66	0.1	0.22	0.02
100m Sand	0.21	0.17	0.28	0.43	0.41	0.48	0.8	0.62	0.65	1.04	1.21	0.84	0.98	1.05	0.87	0.13	0.2	0.07
40m Mud																		
20m Sand	-0.6	-0.5	-1	0.07	0.12	0.02	0.42	0.49	0.32	0.47	0.61	0.38	0.3	0.47	0.22	0.29	0.4	0.15
50m Sand	0.1	0.02	0.6	0.48	0.43	0.49	0.78	0.68	0.85	0.98	0.87	1.05	0.67	0.77	0.73	0.28	0.19	0.5
70m Sand	0.08	0.04	0.46	0.53	0.42	0.55	0.77	0.62	0.9	0.96	0.82	1.03	0.77	0.75	0.86	0.17	0.12	0.21
100m Sand	0.02	0.01	0.05	0.34	0.3	0.42	0.68	0.58	0.73	0.81	0.78	0.84	0.62	0.7	0.68	0.3	0.28	0.43
80m Mud																		
20m Sand	0.18	0.05	0.57	0.37	0.33	0.45	0.61	0.57	0.65	0.72	0.68	0.78	0.79	0.75	0.91	0.2	0.34	0.06
50m Sand	0.42	0.3	0.72	0.2	0.13	0.5	0.39	0.34	0.28	0.59	0.6	0.48	0.77	0.71	0.85	0.06	0.04	0.1
70m Sand	0.44	0.35	0.58	0.24	0.35	0.44	0.39	0.42	0.31	0.61	0.75	0.59	0.78	0.81	0.89	0.11	0.17	0.22
100m Sand	0.43	0.34	0.56	0.35	0.38	0.47	0.39	0.42	0.24	0.63	0.71	0.49	0.74	0.79	0.87	0.08	0.1	0.18

In Figure 4 below where coal seam thickness is plotted on the horizontal axis and the amplitude of tight sandstone beneath the coal is plotted on the vertical axis, the formula for calculating the distance from the predicted point to the gas-bearing sandstone trend line is as follows:

$$l_a = \sqrt{a(x_{A`} \_ x_A)^2 + b(y_{A`} \_ y_A)^2}$$

In this context, la represents the distance from sample point A` to the reference line of tight gas reservoir, with “a” and “b” being normalization constants for distance.
The formula for predicting the hydrocarbon probability of sample points using the inverse distance weighting algorithm is as follows:

$$w_i = l_i^{-p} / \sum_{j=1}^{n} l_j^{-p} \quad \text{,wherein } \sum_{i=1}^{n} w_i = 1$$

$$P(x,y) = \sum_{i=1}^{n} \mathrm{w_i} \;\; P(x_i, y_i)$$

Where w_i represents the weight of sample point i, and P(x,y) represents the predicted hydrocarbon probability of the reservoir at point (x, y).

2.2.2 Research methods and findings

The post-stack hydrocarbon detection based on the coal seam amplitude impact factor is primarily conducted in the prediction section. In this method, the amplitude impact factor of the coal seam on the sandstone is represented by the gas-bearing sandstone trend line, with distance serving as an indicator of the gas probability at reservoir sample points. Figure 4 illustrates the distribution of gas probability in tight sandstone reservoirs below the coal seam, with coal seam thickness plotted on the horizontal axis and amplitude below the coal seam on the vertical axis. The color of points in the figure indicates their distance from the gas-bearing sandstone trend line, which means the probability that can be converted to gas. The figure demonstrates that the shape of the predicted data points closely aligns with the gas-bearing sandstone line, revealing a positive correlation between the amplitude impact factor and coal seam thickness. Warmer color in figure shows predicted sample points with higher gas probability, showing a distribution pattern of the convergence towards the trend line of gas bearing sandstone. Figure 8(a) shows the attribute map of gas probability derived from sandstone amplitude and coal seam thickness, and the prediction results highlight possible gas bearing characteristic of depression area.

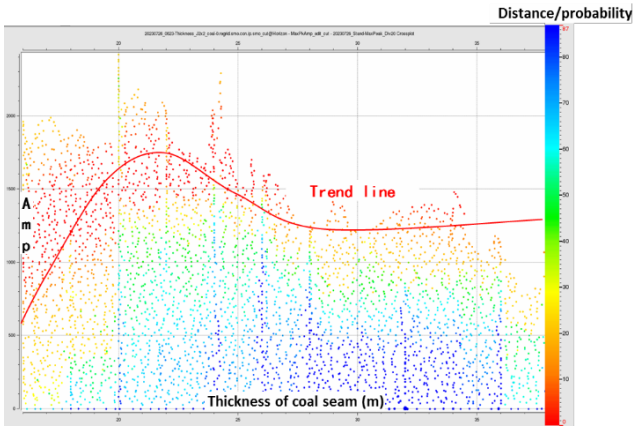

Figure 4 The gas probability distribution map of tight sandstone reservoirs underlying the coal seam.

2.3 Post-stack hydrocarbon detection based on waveform decomposition and reconstruction

2.3.1 Theoretical Framework

When seismic waves pass through underground strata, different rock types and hydrocarbon status of strata shows various responses to seismic signals, leading to differences in the seismic waveforms and frequencies. This principle forms the basis for utilizing frequency information in hydrocarbon detection. The presence of coal seams changes the waveform of the reservoir under the coal seams. While gas-bearing intervals show strong absorption of high-frequency seismic energy, coal seams also show low-frequency characteristics, which reduce the effectiveness of frequency-based hydrocarbon detection. In coal-bearing formations, the hydrocarbon status can be predicted by distinguishing the amplitude of tight sandstone unaffected by coal seams and the amplitude of tight sandstone affected by coal seams, which is based on the amplitude variation of sandstone before and after coal seam development. Areas with enhanced amplitudes indicate higher gas probability. Seismic wave decomposition and reconstruction is a computational method based on the multi-wave seismic trace model, where seismic traces are

decomposed into sets of wavelets with different dominant frequencies, shapes, and positions. By combining wavelet sets across the frequency spectrum, an approximately reconstructed data volume is derived from the original seismic data volume. To characterize the target gas reservoir, specific types of wavelets can be selected for superposition to reconstruct new seismic traces [5].

2.3.2 Research methods and findings

This section of the study focuses on seismic wave decomposition and reconstruction. Figure 5 displays a profile of volume wave decomposition for an oil and gas well, organized by waveform energy. Components 1-6 factors are indicative of strong reflection characteristics of coal seams, while components 7-9 factors and 14-15 factors represent reflections of tight sandstone beneath the coal seam. In Figure 6, a comparison of seismic profiles that crossed the drilling wells in the study area is presented, the original seismic data shows in above and the seismic data reconstructed from volume waveforms shows in below. Through this comparison, the reconstructed profile effectively eliminates the influence of strong side lobes from coal seams, preserving the reflection characteristics of sandstone and shale. It leads to enhanced resolution of the reservoir beneath the coal seam, while the reflection characteristics of other formations remain largely unchanged. By utilizing the reconstructed seismic profile, the amplitude attributes of tight sandstone unaffected by coal seams can be determined. Figure 8 (b) illustrates the distribution of gas-bearing sandstone which was predicted based on the difference between tight sandstone amplitudes before and after volume waveform reconstruction, indicating a high possibility of oil and gas presence in the central and northern regions of the depression area.

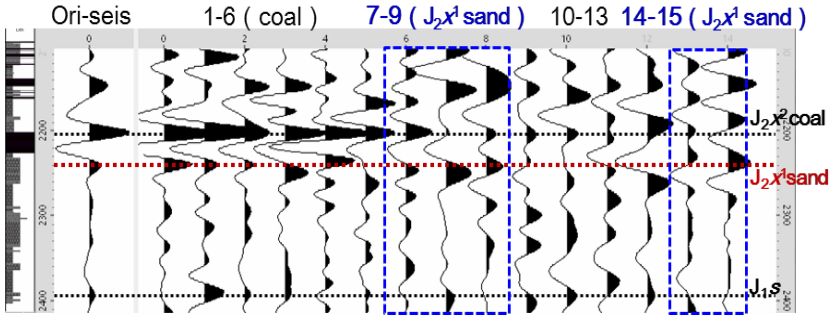

Figure 5 Seismic wave decomposition results in the study area

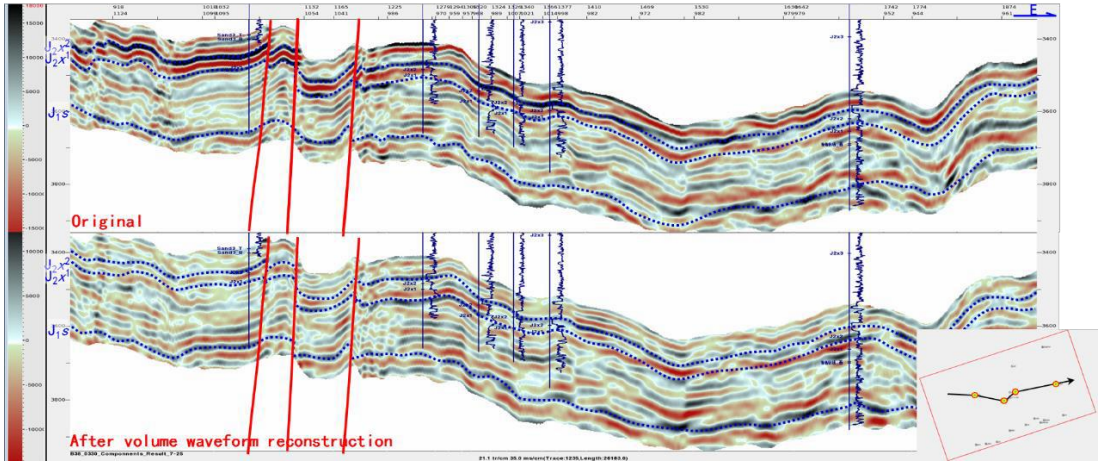

Figure 6 Comparison of well –seismic tie profiles in the study area.

2.4 Post-stack hydrocarbon detection based on absorption attenuation coefficient of coal seams

2.4.1 Theoretical Framework

Due to the imperfect elastic properties of the medium, the amplitude of stress waves experiences attenuation during propagation, leading to energy absorption. Commonly used quantitative measures for characterizing this attenuation include the medium quality factor and the absorption attenuation coefficient α[6-7]. The quality factor describes the imperfect elastic characteristics of the medium and is currently the most commonly used parameter for seismic wave attenuation. It represents the ratio of the energy consumed during propagation over a wavelength distance to the energy before propagation. The quality factor is an intrinsic property of the rock itself. A value approaching 0 indicates strong attenuation, with almost all energy being consumed. Conversely, as the quality factor approaches infinity, it indicates weak attenuation, resembling a state of perfect elasticity. The absorption attenuation coefficient α quantifies the degree of amplitude attenuation of seismic waves after propagating a specific distance. Experimental research on the quality factor is more advanced among all quantitative representations of elastic wave attenuation theories. In field processing, various methods that can withstand noise and accurately determine the quality factor are usually used to calculate the relevant quality factors[8].

In this paper, the quality factor is calculated by the amplitude attenuation method, which only considers the maximum amplitude of the wavelet. The calculation formula is as follows：

$$A(x) = A_0 * \exp\left(-\frac{\pi f}{vQ} * x\right)$$

by transforming:

$$\frac{A(x)}{A(x_0)} = (\frac{x_0}{x})^n * \exp\left[-\frac{\pi f}{vQ} * (x - x_0)\right]$$

Where A(x0) is the amplitude at the reference position x_0, A(x) is the amplitude at the reference position x, x^n is the geometric divergence, and $A'=A_0 * x^n$.

The absorption attenuation coefficient α of the strata can be calculated using the following equation：

$$\alpha = \frac{1}{\Delta x} \ln \frac{A_1}{A_2}$$

Where Δx is the propagation distance in meters; A_1 and A_2 are the initial velocity of the signal and the velocity after propagating a distance of Δx, respectively, in meters per second.

Through the geometric divergence of the quality factor Q, the relationship between α, the quality factor Q, velocity, and frequency can be established. The above relationship can be simplified as：

$$\alpha = K * \frac{\pi f}{Qv}$$

Where f represents the frequency, v is the velocity, and k is a constant.

2.4.2 Research methods and findings

According to the absorption attenuation coefficient, the amplitude of tight sandstone under coal can be restored. Table 2 and Figure 7 illustrate the relationship between the measured curves of a well in the study area and the absorption attenuation coefficient α. Cross-plot analysis reveals a negative correlation between the absorption attenuation coefficient and the longitudinal wave impedance, indicating that higher longitudinal wave impedance results in less amplitude attenuation. By utilizing the absorption attenuation coefficient of the coal seam for anti-filtering, the coal seam reflection can be eliminated, and the amplitude characteristics of tight sandstone before coal seam influence could be extracted. This information can be used to predict potential gas- bearing zones based on amplitude variations. Figure 8(c) displays the anticipated distribution of gas-bearing sandstone which is predicted by the absorption attenuation coefficient of the coal seam, and the prediction result shows that gas-bearing zones are predominantly located in the eastern and northern regions of the depression.

Table 2 Comparison of the basic parameters and absorption attenuation coefficients of different formations.

Lith	Depth	Velocity (m/s)	Densityρ ($g*cm^{-3}$)	Absorption attenuation coefficientα (m^{-1})	P- impedance ($m/s*g*cm^{-3}$)
shale1	4145	3793	2.52	0.28	9558
coal1	5088	3290	1.4	0.31	4606
sand1	5145	5100	2.6	0.23	13260
coal2	5182	2900	1.17	0.36	3393
sand2	5250	4900	2.56	0.24	12544
shale2	5310	4030	2.68	0.27	10800
sand3	5335	5330	2.59	0.22	13805

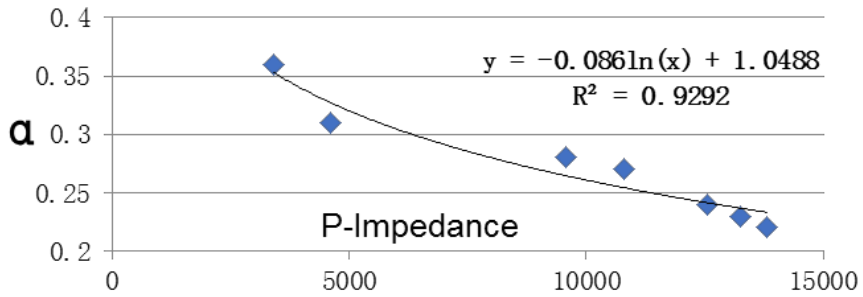

Figure 7 Crossplot of longitudinal wave impedance and coal seam absorption attenuation coefficient.

3 Application effect

The above three meothods all utilize the differences in amplitude before and after the presence of oil and gas in the coal reservoir to conduct post-stack hydrocarbon detection. Among them, the prediction method based on the amplitude impact factor of the coal seam relies on the inversion of geological statistics to obtain the thickness of the coal seam, the shale below the coal, and the sandstone below the coal. This method determines the hydrocarbon properties of the reservoir through the probability distribution map of gas-bearing tight sandstone under the coal seam. The reliability of the prediction results is higher when the total thickness of the shale and tight sandstone under the coal seam is greater than 1/4 wavelength and less than 1/2 wavelength.

The prediction method based on seismic signal decomposition and reconstruction utilizes volume wave decomposition to strip off the coal seam in the post-stack seismic data and conducts oil and gas detection based on the amplitude differences of the coal reservoir before and after reconstruction. This method requires fewer intermediate processes, resulting in more reliable prediction results.

The prediction method based on the absorption attenuation coefficient of the coal seam eliminates the influence of the coal seam on the underlying strata by anti-filtering the post-stack seismic data. By calculating the amplitude differences of the coal reservoir before and after filtering, the oil and gas status can be predicted, with the key point being the accurate determination of the Q factor of the coal seam. Comparison of the results of post-stack oil and gas detection using these three methods reveals that the predicted gas-bearing areas are predominantly located in the eastern and northern parts of the depression, with the similarity of these results exceeding 80%. The predicted hydrocarbon distribution area correlates closely with the nose-shaped structures in the lower depression area and the oil and gas status of drilled wells. These findings offer dependable research outcomes for the identification of geological sweet spots and the formulation of exploration and development strategies.

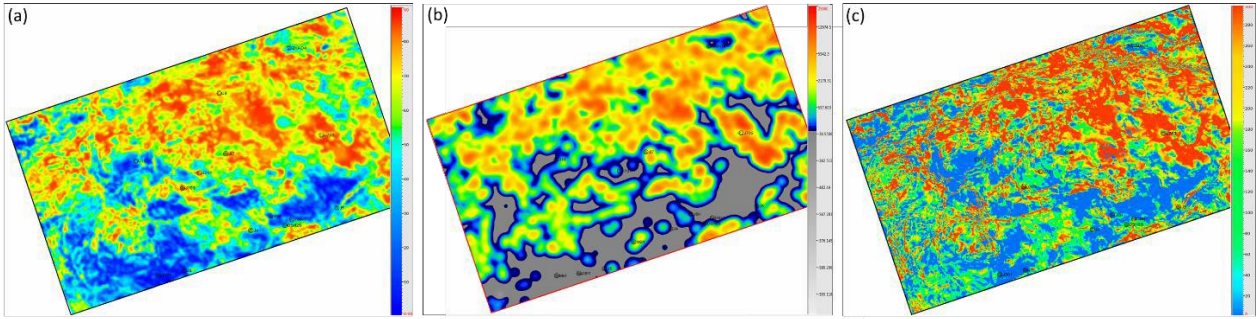

Figure 8 Comparative of the prediction results from three post-stack oil and gas detection methods.
（a: Hydrocarbon detection map based on the amplitude influence factor of the coal seam b: Hydrocarbon detection map based on seismic wave decomposition and reconstruction c: Hydrocarbon detection map based on the absorption attenuation coefficient of the coal seam）

4 Conclusion and Insights

1） In the study of coal-bearing strata, forward analysis is fundamental. Although the strong energy of coal seam has potential interference on the response characteristics of oil and gas reservoirs, understanding and utilizing its influence are helpful to predict the oil and gas properties of underlying tight sandstone reservoirs.

2） The amplitude impact factor, rooted in statistical-probabilistic theory, predicts the probability of oil and gas presence by analyzing the trend line of gas-bearing sandstone and the amplitude enhancement characteristics after gas pooling in underlying tight sandstone. This method minimizes the loss of effective signals during coal seam removal and reduces systematic errors caused by attribute transformations. While the prediction results can be optimized from a geological perspective and offer strong controllability, they are subject to certain limitations.

3） Both the methods based on volume wave decomposition & reconstruction and absorption attenuation

coefficient are used for oil and gas detection by filtering out coal seam signals. However, this filtering process may compromise some information of the sandstone below the coal seam, leading to limitations and potential systematic errors in predicting sandstone reflection under coal-free conditions. Nevertheless, the advantage of these methods lies in their broad applicability. Despite the different theoretical foundations of the three methods discussed in the paper, the high similarity of these three prediction results effectively supports production, demonstrates strong generalizability, and holds significant importance for the efficient exploration and development of tight sandstone oil and gas reservoirs under strong energy shielding.

References

U.S. Energy Information Administration. Annual Energy Outlook 2012 [R]. Washington: U.S. Energy Information Administration, 2012.

Marc S. Hendrix, et al. AAPG Bulletin[C]. Sedimentology, organic geochemistry, and petroleum prospects of the Jurassic coal-bearing strata in the three major basins in Northwest China. Vol.79, No.7, 1995.

Kuang Lichun, Zhi Dongming, Wang Xiaojun, et al. Oil and gas accumulation assemblages in deep to ultra- deep formations and exploration targets of petroliferous basins in Xinjiang region[J]. China Petroleum Exploration, 2021,26(4):1-16.

Liang Shijun, Qian Feng, Xiao Dongsheng. Exploration discovery and implications of the Jurassic tight sandstone oil and gas reservoir in Well Ji7H in Taibei Sag, Turpan-Hami Basin [J]. China Petroleum Exploration, 2022, 27 (1):50-59.

Castagna J P, Sun S J, Siegfried R W. Instantaneous Spectral analysis: detection of low-frequency shadows associated with hydrocarbons[J]. The Leading Edge, 2003, 22(2):120-127.

White J E. Computed seismic speeds and attenuation in rocks with partial gas saturation. Geophysics, 1975, 40(2):224-232.

Carcione J M, Cavallini F. Attenuation and quality factor surfaces in anisotropic-viscoelastic media [J].
Mechanics of Materials, 1995, 19(4):311-327.

Tang Shilei. The Study on the Relationship between the Attenuation and the Reflection Coefficient in Sulige Tight Gas Reservoirs. [D].
China university of petroleum (Beijing), 2020.